Pol. J. Environ. Stud. Vol. 31, No. 4 (2022), 3745-3753
DOI: *10.15244/pjoes/147198* ONLINE PUBLICATION DATE: 2022-05-20

Original Research

Influence of *In-situ* Soil and Groundwater Level on Hydrological Effect of Bioretention

Junkui Pan[1]*, Ruiqiang Ni[2], Longfei Zheng[3]

[1]School of Civil and Transportation Engineering, Henan University of Urban Construction, Longxiang Avenue, Xinhua District, Pingdingshan 467000, China
[2]China Railway 10th Bureau Group Investment Development Co., Ltd, China Railway Caizhi Industrial South Road, Lixia District, Jinan 250001, China
[3]Pingdingshan Highway Development Center, Jiaotong building, Chang'an Avenue, Xinhua District, Pingdingshan 467000, China

Received: 8 January 2022
Accepted: 7 March 2022

Abstract

Bioretention is an important technology for ecological control of runoff. The purpose of this study was to investigate the coupling effect of *in-situ* soil and groundwater level on the hydrological performance of bioretention. VADOSE/W was used to simulate the water transport processes during bioretention under a single rainfall event. The effects of four *in-situ* soil types and two groundwater levels on the surface ponding, underdrain outflow, exfiltration, and runoff regulation effects of bioretention were studied. Under eight geological situations and the rainfall of 0.17 mm/h (6.0 h), the ponding duration and overflow volume of bioretention were 556-649 min and 24.71-39.61 mm/m^2, respectively; the underdrain outflow peak value and duration were 0.549-0.804 mm/min and 380-730 min, respectively; the exfiltration volume per unit area from the bottom and lateral of bioretention were 106.79-396.10 mm/m^2 and 50.60-147.45 mm/m^2, respectively; and the runoff reduction rate, runoff peak reduction rate, and runoff delay time of bioretention were 53.46%-96.19%, 18.43%-68.08%, and 288-318 min, respectively. These results suggest that bioretention without an underdrain and with a relatively smaller K_s (saturated permeability coefficient) of *in-situ* soil might result in longer ponding times and larger overflow volumes. With an increase in K_s of *in-situ* soil, the underdrain outflow weakens, the exfiltration volume increases, and the runoff control effects improve. Although the groundwater level has little effect on surface ponding, it can cause a stronger underdrain outflow. The shallower groundwater level leads to a larger exfiltration volume when the K_s of in-soil is much smaller than that of the planting layer and leads to a reduced runoff regulation effect for bioretention without an underdrain. Therefore, when locating and designing bioretention systems, the *in-situ* soil type and groundwater level should be comprehensively considered to ensure that the runoff control target is achieved.

Keywords: bioretention, hydrological effect, *in-situ* soil, groundwater level, VADOSE/W

*e-mail: 15303950218@163.com

Introduction

With the acceleration of global urbanisation, the impervious area of urban areas has increased sharply, resulting in a significant reduction in rainwater infiltration. This shortens the concentration time of rainfall and increases the peak of runoff, causing frequent urban waterlogging [1-3]. Moreover, the groundwater in urban areas cannot be effectively recharged, causing the groundwater level to decline year by year [4-6]. In addition, urban surface runoff usually contains pollutants, such as nutrients, heavy metals, suspended solids, petroleum, hydrocarbons, pathogens and salts, which flow into the downstream water system through the urban rainwater pipe network and pose serious adverse impacts on the regional water environment, and also threaten human health [7-12].

As the global water environment continues to deteriorate, some technical measures have emerged to solve urban water problems, such as permeable pavement, green roof, grassed swales, bioretention, constructed wetland and stabilization pond [13-19]. Among them, bioretention integrates landscape, flexible layout, runoff control, and water purification functions and has emerged as a promising and practical rainwater ecological control measure [20-22]. A typical bioretention system is usually composed of a 15-30 cm surface aquifer layer, a 5-8 cm mulch layer, a 30-70 cm planting filler layer, a 15-30 cm sandy gravel layer, an overflow hole, and plants, and the design scale is generally 5-10% of the catchment area (Fig. 1) [23-25]. An underdrain with a diameter of 50-100 mm is usually installed in the sandy gravel layer to strengthen the drainage of bioretention when the *in-situ* soil permeability coefficient is lower than 1.27 cm/h or the bioretention system is anti-seepage [26]. To control rainwater runoff, when rainwater runoff flows through the bioretention system, the planting filler layer intercepts and stores the water, with part of it slowly penetrating into the surrounding soil to recharge the groundwater and the rest diffusing into the atmosphere through evaporation and plant transpiration after rainfall [27-28].

In recent years, the hydrological performance of bioretention systems has been extensively studied through laboratory and field experiments. Davis [29], Pan [30], and Debusk [31] have demonstrated that bioretention can regulate rainfall runoff and improve the regional hydrological cycle. Some studies have shown that the hydrological effects of bioretention are mainly affected by factors such as rainfall characteristics and bioretention design parameters. For example, both Gülbaz [32] and Gao [33] showed that increasing the rainfall intensity or duration increased the surface ponding depth and outflow peak flow rate of bioretention. Li [34] reported that amount of water infiltration increased with the depth of the planting filler layer, and the goal of LID (low-impact development) was achieved more easily. Both Li [35] and Brown [36] demonstrated that by setting up internal water storage areas, bioretention could better reduce runoff volume and runoff peak, extend runoff retention time, and improve hydrological performance.

The numerical model can provide support for the planning, design, and research of water ecological treatment systems [37]. At present, only a few hydrologic models, such as RECARGA, HYDRUS-1D, SWMM, and SUSTAIN, are available to simulate storm-water runoff management of bioretention. The RECARGA model uses the Green-Ampt equation to represent infiltration, which is specifically designed for bioretention. However, it is mainly suitable for long-term water balance analysis and not for simulating the water transport process of bioretention under short-term rainfall. Moreover, it is unable to arbitrarily specify the hydraulic parameters of the medium, which limits

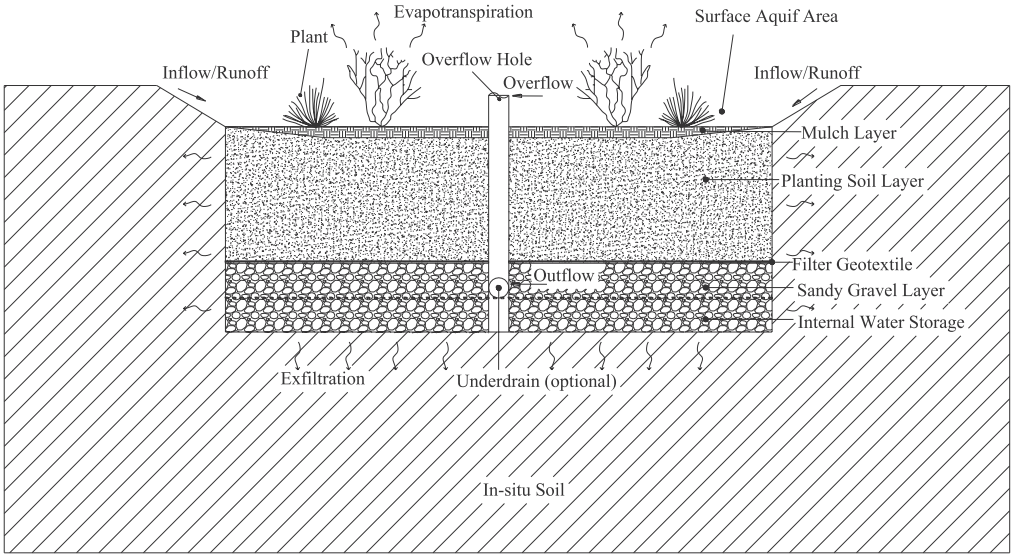

Fig. 1. Cross-sectional diagram of a typical bioretention cell.

its wide application [38]. The HYDRUS-1D model adopts Richards' equation to simulate water movement in soil. However, it is a one-dimensional model that does not consider the lateral diffusion of soil water, so it is not suitable for bioretention with an internal water storage area and to simulate horizontal exfiltration *in-situ* soil [39]. SWMM and SUSTAIN are used to simulate the runoff process and plan the LID measures for the entire region, simplifying the structural design parameters and water infiltration process of bioretention. Both of these models have notable shortcomings when studying bioretention alone [40-41]. VADOSE/W is a two-dimensional numerical model that is used to simulate soil seepage, groundwater change, evaporation, and plant transpiration under saturated or unsaturated conditions. It is coupled with Richards' equation and atmospheric boundary conditions to calculate soil water movement and surface ponding processes on the soil [42]. Gao [33] used the VADOSE/W model to study the ponding and outflow processes of road bioretention and proved that it could effectively simulate the hydrological effects of two-dimensional bioretention.

Bioretention has recently become popular in various regions to address rainwater problems effectively. However, the differences in *in-situ* soil and groundwater level in different regions may have an impact on the operational effect of bioretention. For example, both Gao [43] and Boancă [44] proved that *in-situ* soil texture was an important element of control in the design and performance of bioretention cells. Line [45] demonstrated through the field tests that the contribution of groundwater might be an important reason for the outflow of bioretention being greater than the inflow. Therefore, the expected runoff control objectives may not be achieved if the bioretention is set without considering the local geological situation. However, research on the coupling effect of *in-situ* soil and groundwater level on the hydrological performance of bioretention is limited.

The objective of this study was to use the two-dimensional numerical model VADOSE/W to simulate the water transport process of bioretention media and *in-situ* soil in the saturated-unsaturated state and to study the coupling influence of *in-situ* soil type and groundwater level on the hydrological effects of bioretention (such as surface ponding, underdrain outflow, exfiltration, and runoff regulation) to provide a reference for the application of bioretention in different areas.

Material and Methods

Governing Equation of Soil Water Movement

As the bioretention medium and *in-situ* soil belong to variably saturated soil, including vertical and horizontal water diffusion, their water movement processes can be described by the two-dimensional Richards' equation, as shown in Eq. (1).

$$\frac{\partial\theta}{\partial t}=\frac{\partial}{\partial x}\left[k(\theta)\frac{\partial h}{\partial x}\right]+\frac{\partial}{\partial z}\left[k(\theta)\frac{\partial h}{\partial z}\right]+\frac{\partial k(\theta)}{\partial z}-S(x,z,t) \quad (1)$$

where h is the soil negative pressure head (mm); $k(\theta)$ is the soil permeability coefficient (mm/min); θ is the soil volumetric moisture content (mm^3/mm^3); x and z are the horizontal and vertical positions, respectively (mm); $S(x, z, t)$ is the source and sink terms, such as evapotranspiration (mm/min), which can be taken as 0 when the duration is short; and t is the time (min).

When $h\geq 0$, the soil is saturated, and θ and $k(\theta)$ in Equation 1 are both fixed values, which are the saturated soil water content θ_s and the saturated soil permeability coefficient K_s, respectively. When $h<0$, the soil is in unsaturated, and θ and $k(\theta)$ are variable values, which can be described by the soil water characteristic curve formula (Eq. 2) and the hydraulic conductivity curve formula (Eq. 3), respectively, as proposed by van Genuchten [46].

$$\theta(h)=\begin{cases}\theta_r+\dfrac{\theta_s-\theta_r}{\left[1+|ah|^n\right]^m} & (h<0)\\ \theta_s & (h\geq 0)\end{cases} \quad (2)$$

$$K(\theta)=\begin{cases}K_s S_e^{1/2}\left[1-\left(1-S_e^{1/m}\right)^m\right]^2 & (h<0)\\ K_s & (h\geq 0)\end{cases} \quad (3)$$

where θ_r is the residual soil water content (mm^3/mm^3); θ_s is the saturated soil water content (mm^3/mm^3); a, n, and m are the van Genuchten parameters, and $m = 1 - 1/n$; K_s is the saturated soil permeability coefficient (mm/min); S_e is the effective saturation of soil water, and $S_e = (\theta - \theta_r)/(\theta_s - \theta_r)$.

Design Rainfall

The determination of the design rainfall is necessary to study the hydrological effects of bioretention. The design rainfall adopted in this study is the once-a-year 6 h design rainfall calculated according to the rainstorm intensity formula in the study area (Eq. 4) in which the rainfall intensity is 0.17 mm/min, and the total rainfall is 62.59 mm, which is a uniform rainfall type, to ensure that the water penetrates the bioretention filler layer and *in-situ* soil with sufficient time and water volume.

$$q=\frac{15.054\left(1+0.845\lg P\right)}{\left(t+14.095\right)^{0.753}} \quad (4)$$

where q is the rainfall intensity (mm/min); t is the rainfall time (min); and P is the rainfall return period (a).

The runoff entering bioretention system is mainly composed of the runoff in the catchment area and the rainfall directly acting on bioretention, which can be calculated using Eq. (5).

$$q_0 = \frac{q\left(\Psi F_0 + F_1\right)}{F_1} \tag{5}$$

where q_0 is the runoff intensity acting on bioretention (mm/min); q is the actual rainfall intensity (mm/min); Ψ is the runoff coefficient, which is taken as 0.9 in this study; F_0 is catchment area (m^2); and F_1 is the bioretention area (m^2).

Simulated Scenarios

To study the hydrological performance of bioretention under the coupling effect of *in-situ* soil and groundwater level, the VADOSE/W model was used to simulate the water transport process of bioretention under eight geological situations, as shown in Table 1. Four types of *in-situ* soil, including silty loam (SL), loam (L), sandy clay loam (SCL), and sandy loam (SaL), and two types of groundwater levels, 1 m and 3 m below the bottom of the bioretention, were adopted. Different parameters considered for bioretention under various geological conditions include: 10% of the catchment area, the surfer aquifer depth of 20 cm, the mulch layer thickness of 5 cm, the planting filler layer thickness of 70 cm, and the sandy gravel layer thickness of 30 cm. When the *in-situ* soil was silty loam or loam, an underdrain with a diameter of 5 cm was placed in the middle of the sandy gravel layer to form an internal water storage with a height of 15 cm because its permeability coefficient was lower than 1.27 cm/h. The simulation time of this study was short, and the amount of evaporation and plant transpiration could be ignored. Therefore, the influence of plants was not considered. In addition, the mulch layer of bioretention usually adopts crushed bark or gravel, which has a large permeability coefficient and can be regarded as an aquifer on the planting soil layer. Therefore, the mulch layer is not considered in the simulation, but only its effective pores can be superimposed on the original aquifer. In this study, the depth of the aquifer was 20 cm, which was the depth at which the superposition of the pores of the mulch was considered.

Soil Hydraulic Characteristic Parameters

The soil hydraulic characteristic parameters of the bioretention medium and *in-situ* soils for the VADOSE/W model are shown in Table 2. In this study, the soil hydraulic characteristic parameters of planting filler and sandy gravel in bioretention are based on the data verified in our previous study when studying the influence of bioretention parameters on the road runoff regulation effect [33], whereas *in-situ* soils use the data used by Li when studying water unsaturated seepage in rainwater seepage ditch [47]. In addition, the initial water contents of the bioretention medium and *in-situ* soils are the water content distributions after the free drainage of the medium reaches stability under the saturated state.

Data Analysis

The regulation effect of bioretention on a single rainfall event can be described by three indicators: runoff volume reduction rate, runoff peak reduction rate, and runoff delay time, as shown in Eqs (6)-(7), and (8), respectively.

$$R_V = \frac{V_{in} - V_{out}}{V_{in}} \times 100\% \tag{6}$$

Table 1. Bioretention design parameters and geological situations.

Simulated scenarios	Bioretention design parameters					Geological situations	
	$A_{bioretention}/A_{catchment}$ (%)	Aquifer depth (cm)	Thickness of planting filler layer (cm)	Thickness of sandy gravel layer (cm)	Height of internal water storage (cm)	*In-situ* soil type	Distance between groundwater level and bioretention bottom (m)
SL-1	10	20	70	30	15	Silt loam	1
SL-3					15	Silt loam	3
L-1					15	Loam	1
L-1					15	Loam	3
SCL-1					No	Sandy clay loam	1
SCL-3					No	Sandy clay loam	3
SaL-1					No	Sandy loam	1
SaL-3					No	Sandy loam	3

Table 2. Hydraulic characteristic parameters of bioretention medium and in-situ soil

Soil type	K_s (cm/h)	θ_r (cm³/cm³)	θ_s (cm³/cm³)	a (cm^{-1})	n	m
Bioretention medium						
Planting filler	5.041	0.058	0.41	0.057	2.00	0.50
Sandy gravel	163.00	0.046	0.44	0.153	2.64	0.62
In-situ soil						
Silt loam	0.452	0.067	0.45	0.020	1.41	0.29
Loam	1.038	0.078	0.43	0.036	1.56	0.36
Sandy clay loam	1.310	0.100	0.39	0.059	1.48	0.32
Sandy loam	4.428	0.065	0.41	0.075	1.89	0.47

$$R_{peak} = \frac{q_{peak-in} - q_{peak-out}}{q_{peak-in}} \times 100\% \quad (7)$$

$$R_{delay} = t_{out} - t_{in} \quad (8)$$

where R_V is the runoff volume reduction rate (%); V_{in} is the inflow volume (mm); V_{out} is the outflow volume (including overflow and underdrain outflow, mm); R_{peak} is the runoff peak reduction rate (%); $q_{peak-in}$ is the inflow peak value (mm/min); $q_{peak-out}$ is the outflow peak value (mm/min); t_{out} is the time at which bioretention begins to outflow; t_{in} is the time at which the runoff enters the bioretention; and R_{delay} is the runoff delay time (min).

Results and Discussion

Influence of *in-situ* Soil Type and Groundwater Level on Surface Ponding

The range of surface ponding duration and overflow volume are two important indicators of surface ponding bioretention. As shown in Table 3, for bioretention under eight geological situations, the range of these indicators are 556-649 min and 24.71-39.61 mm/m², respectively. The *in-situ* soil type and the underdrain have a significant impact on the surface ponding, but the impact of the groundwater level is not significant.

Compared with SL and L, the surface ponding duration and overflow volume of bioretention increases to 86 minutes and 6.66 mm/m², respectively, under SCL. This is because the K_s (1.310 cm/h) of SCL is much smaller than that of the planting filler layer (5.040 cm/h), and it is not equipped with an underdrain. Therefore, the water infiltrating into bioretention easily accumulates at the bottom of the bioretention and enters the planting filler layer, which affects the infiltration of rainwater, significantly prolongs the ponding time, and increases the overflow volume. Although the underdrain is not installed, the K_s (4.428 cm/h) of SaL is close to that of the planting filler, so the water is more easily diffused to the *in-situ* soil, resulting in a relatively shorter surface ponding duration (reduced by up to 93 min) and a significantly smaller overflow volume (reduced by up to 14.90 mm/m²) than SCL.

Table 3. Surface ponding of bioretention under different *in-situ* soil types and groundwater levels.

Simulated scenarios	Time of surface ponding beginning (min)	Time of surface ponding ending (min)	Duration of surface ponding (min)	Maximum surface ponding depth (cm)	Time of overflow occurring (min)	Time of overflow ending (min)	Overflow volume (mm/m²)
SL-1	8	563	555	20	305	300	35.34
SL-3	3	563	560	20	304	300	35.24
L-1	8	562	554	20	308	300	32.95
L-3	8	562	554	20	308	300	32.15
SCL-1	9	649	640	20	309	300	39.61
SCL-3	9	614	605	20	308	300	38.49
SaL-1	8	556	548	20	318	300	24.71
SaL-3	9	556	547	20	318	300	23.85

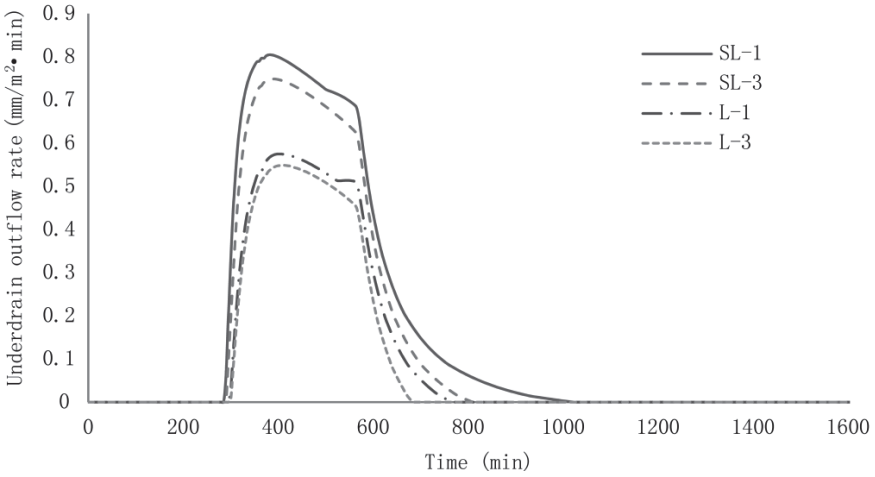

Fig.2. Underdrain outflow rate of bioretention under different *in-situ* soil types and groundwater levels.

Influence of *in-situ* Soil Type and Groundwater Level on Underdrain Outflow

As shown in Fig. 2, compared with rainfall runoff, under four geological situations, the underdrain outflow start time of bioretention is delayed by 290-300 min, the end time is delayed by 320-660 min, and the outflow peak value is reduced by 53.72-68.42%. Rainwater runoff can be temporarily stored and then slowly released through the infiltration process of the planting filler of bioretention, which has a significant delay and peak elimination effect.

The order of the underdrain outflow start time is L-1 and L-3>SL-1 and SL-3, and the order of the outflow peak value and end time are both SL-1>SL-3>L-1>L-3. The *in-situ* soil type have a significant impact on the underdrain outflow; i.e., with the increase in the K_s of *in-situ* soil, the start time of the underdrain outflow is delayed, the peak value is decreased, and the end time is earlier. In addition, the groundwater level has little effect on the start time of the underdrain outflow, but shallower groundwater levels tend to lead to relatively larger outflow peaks and longer outflow durations. Furthermore, compared with L, the influence of groundwater level on underdrain outflow is more significant as the *in-situ* soil is SL, which has a relatively smaller K_s.

Influence of *in-situ* Soil Type and Groundwater Level on Exfiltration

As shown in Figs 3a) and 3b), the lateral and bottom accumulated exfiltration volume of bioretention gradually increases and tends to be stable over time. Moreover, the time of stability reaches earlier with the increasing K_s of *in-situ* soil. The exfiltration volume per unit area from the bottom and lateral of bioretention is 106.79-396.10 mm/m^2 and 50.60-147.45 mm/m^2, respectively, and the bottom can reach 1.72-7.82 times the lateral, 24 hours after the end of rainfall, under eight geological situations.

The K_s of *in-situ* soil plays a leading role in bottom exfiltration; i.e., with the increase in the K_s of *in-situ* soil, the bottom exfiltration volume increases significantly. The order of cumulative exfiltration volume of bioretention is SaL-1 and SaL-3>SCL-3> SCL-1>L-3>L-1>SL-3>SL-1. The influence of the groundwater level on bottom exfiltration differs according to the *in-situ* soil type. When the *in-situ* soil is SL, L, or SCL, the shallower groundwater level tends to result in a smaller exfiltration volume, whereas when

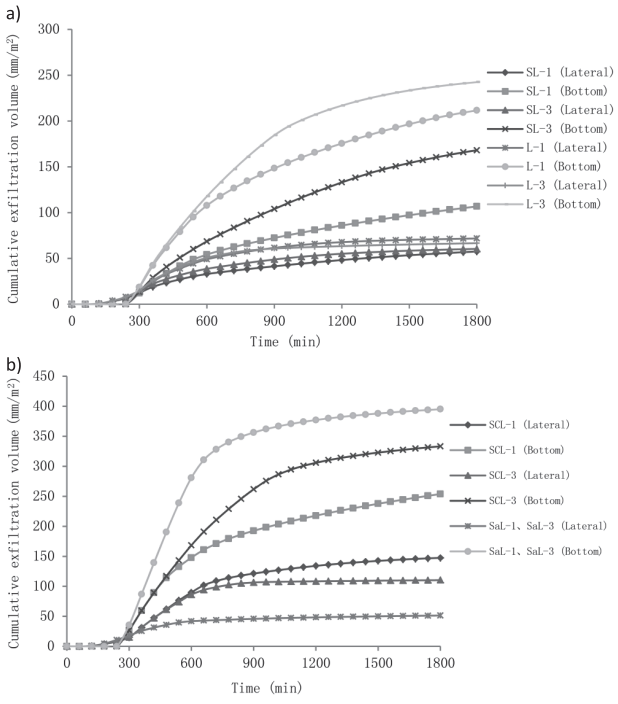

Fig. 3. Cumulative exfiltration volume of bioretention under different *in-situ* soil types and groundwater levels: a) bioretention with an underdrain, b) bioretention without an underdrain.

the *in-situ* soil is SaL, there is almost no effect. This may be due to the larger K_s of sandy loam, and the water infiltrated into the *in-situ* soil can quickly spread to both sides. Therefore, the groundwater level has no obvious effect on the bottom penetration capacity of bioretention.

For lateral exfiltration, the order of the cumulative exfiltration volume of bioretention is SCL-1>SCL-3 >L-1>L-3>SL-3>SL-1>SaL-1 and SaL-3. The lateral exfiltration volume of the SCL is relatively larger, mainly because the K_s of SCL is much smaller than that of the planting filler, and the underdrain is not set. Therefore, the water easily accumulates at the bottom of the bioretention, thus increasing the lateral exfiltration. In addition, the influence of the groundwater level on lateral exfiltration is relatively weaker than that of bottom exfiltration.

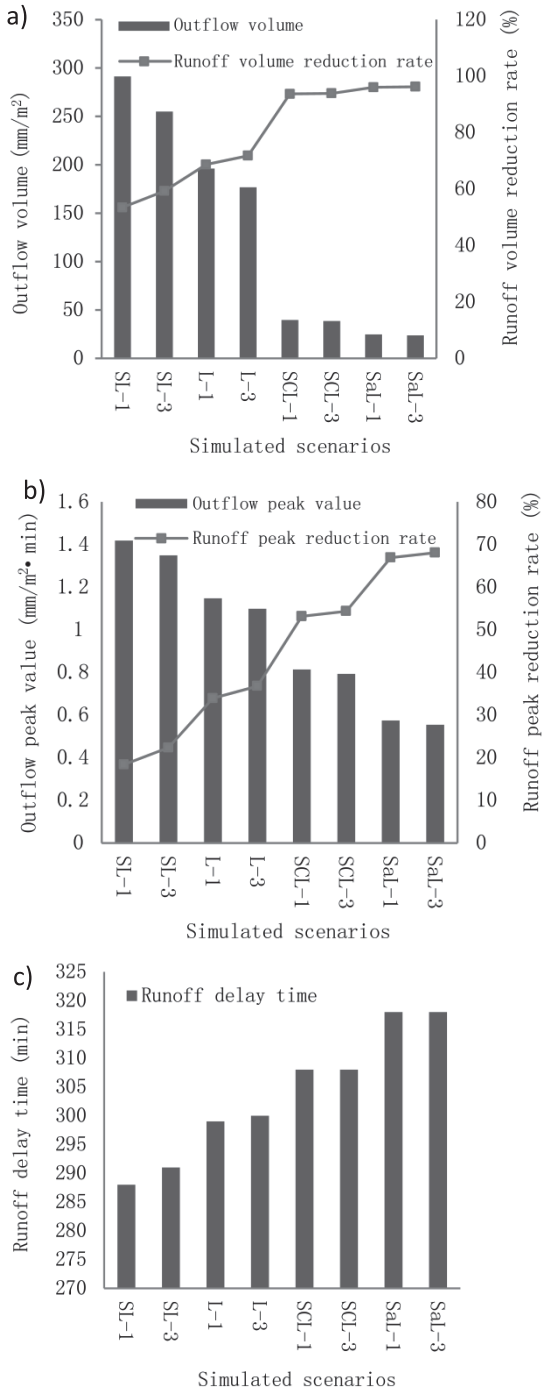

Fig. 4. Runoff regulation effect of bioretention under different *in-situ* soil types and groundwater levels: a) runoff volume reduction, b) runoff peak reduction, and c) runoff delay time.

Influence of *in-situ* Soil Type and Groundwater Level on Runoff Regulation Effect

As shown in Figs 4a) and 4b), the ranges of R_V and R_{peak} of bioretention under the eight geological situations are 53.46-96.19% and 18.43-68.08%, respectively. The order of the R_V and R_{peak} are both SaL-1 and SaL-3>SCL-1 and SCL-3>L-3>L-1>SL-3>SL-1, which are significantly affected by the *in-situ* soil type; i.e., with the increase in K_s of *in-situ* soil, the R_V and R_{peak} both increase. In addition, the shallower groundwater level tends to result in a relatively smaller R_V and R_{peak} when the *in-situ* soil is SL and L (with underdrain), whereas the influence can be ignored when the *in-situ* soil is SCL and SaL (without underdrain). This is mainly because the groundwater level has a significant influence on the underdrain outflow, and the influence on surface overflow is weak. As shown in Fig. 4c), the range of R_{delay} of bioretention under the eight geological situations is 288-318 min, and the order of the R_{delay} is SaL-1 and SaL-3>SCL-1 and SCL-3>L-1 and L-3>SL-1 and SL-3. The R_{delay} is significantly affected by the *in-situ* soil type, as it significantly increases with the increase in K_s of *in-situ* soil. However, the influence of the groundwater level can be ignored.

Conclusion

VADOSE/W was used to study the influence of *in-situ* soil type and groundwater level on the hydrological performance of bioretention under a single rainfall event. The following conclusions were drawn:

For the *in-situ* soil with a much smaller K_s (such as SCL), an underdrain should be configured to reduce overflow risk. The smaller K_s of *in-situ* soil and shallower groundwater level is more likely to lead to the enhancement of underdrain outflow. The exfiltration of bioretention is dominated by bottom seepage, which increases with the increase in K_s of *in-situ* soil. For *in-situ* soil with a much smaller K_s, the shallower groundwater level is more likely to reduce the exfiltration volume. The runoff control effect of bioretention is significantly improved with the increase in K_s of *in-situ* soil. For bioretention with an underdrain, the shallower groundwater level is more likely to weaken the runoff control effect of bioretention.

The results suggest that when locating and designing bioretention, native soil types and groundwater levels should be carefully considered to ensure that the runoff

control target is achieved. In addition, this study only considered a single rainfall event, and the impact of *in-situ* soil type and groundwater level on the long-term hydrological performance of bioretention should be further studied.

Acknowledgments

This work is supported by the National Natural Science Foundation of China (No. 51378520) and the National Natural Science Foundation of Chongqing (No. cstc2018jcyjAX0445).

Conflict of Interest

This manuscript has not been published or presented elsewhere in part or in entirety and is not under consideration by another journal. We have read and understood your journal's policies, and we believe that neither the manuscript nor the study violates any of these. There are no conflicts of interest to declare.

References

1. MATTEO M.D., LIANG R.L., MAIER H.R., THYER M.A., SIMPSON A.R., DANDY G.C., ERNST B. Controlling rainwater storage as a system: An opportunity to reduce urban flood peaks for rare, long duration storms. Environmental Modelling & Software, **111**, 34, **2019**.
2. ANGRILL S., PETIT-BOIX A., MORALES-PINZON T., JOSA A., RIERADEVALL J., GABARRELL X. Urban rainwater runoff quantity and quality – A potential endogenous resource in cities? Journal of Environmental Management, **189** (15), 14, **2017**.
3. JEMBERIE M.A., MELESSE A. M. Urban flood management through urban land use optimization using LID techniques, city of Addis Ababa, Ethiopia. Water, **13**, 1721, **2021**.
4. LI H.E., JIA B.K., CHENG B., GUO C., LI J.K. Research progress on the effect of concentrated runoff infiltration on soil and groundwater in sponge city. Advances in Water Science, **30** (4), 589, **2019** [In Chinese].
5. WANG Z.G., GUO Q.Z., LIAN J.J., CHEN L. Concept and assessment of utilizing rooftop rainwater for pressurized groundwater recharge. Journal of Hydraulic Engineering, **50** (8), 999, **2019** [In Chinese].
6. AMEEN A., JABEEN F., QADIR S. A., AHMED M., ROOM A. Water sensitive urban design for rain water harvesting and groundwater recharge. Advances in Bioresearch, **11** (5), 13, **2020**.
7. OLAL F.O. Assessment of the impact of urban runoff from Migori town on the concentration levels of selected heavy metals in Migori river, Kenya. Journal of Environment and Earth Science, **5** (20), 24, **2015**.
8. DU X.L., ZHU Y.J., HAN Q., YU Z.Y. The influence of traffic density on heavy metals distribution in urban road runoff in Beijing, China. Environmental Science and Pollution Research, **26**, 886, **2018**.
9. RDULESCU D., RACOVIEANU G., PIENARU A. Urban storm water runoff pollution – an overview and recent trends. 3rd International Conference Water 2016 - Ovidius University, **2016**.
10. ANDERSSON M., EGGEN O. A. Urban contamination sources reflected in inorganic pollution in urban lake deposits, Bergen, Norway. Environmental Science: Processes and Impacts, **17** (4), 854, **2015**.
11. FARROKHI M., NAIMI-JOUBANI M., DARGAHI A., POURSADEGHIYAN M., JAMALI H.A. Investigating activated sludge microbial population efficiency in heavy metals removal from compost leachate. Polish Journal of Environmental Studies, **27** (2), 623, **2018**.
12. ALMASI A., MAHMOUDI M., MOHAMMADI M., DARGAHI A., BIGLARI H. Optimizing biological treatment of petroleum industry wastewater in a facultative stabilization pond for simultaneous removal of carbon and phenol. Toxin Reviews, **40** (7), 1, **2019**.
13. WANG M., ZHANG D. Q., SU J., DONG J.W., TAN S.K. Assessing hydrological effects and performance of low impact development practices based on future scenarios modeling. Journal of Cleaner Production, **179** (1), 12, **2018**.
14. WASIM J., NINE A. Adapting cities for climate change: an assessment of green roof technology. International conference on Anthropology, Adaptation and Resilience in Climate Change Regime, October 22-23, 2016, DU, Dhaka, Bangladesh. **2016**.
15. KAMALI M., DELKASH M., TAJRISHY M. Evaluation of permeable pavement responses to urban surface runoff. Journal of Environmental Management, **187** (1), 43, **2017**.
16. GAO J.P., PAN J.K., TANG R.Y., GUO, S.S., LIU Y. LID facility layout and hydrologic impact simulation in an expressway service area. Polish Journal of Environmental Studies, **28** (6), 4153, **2019**.
17. SHAFIQUE M. A review of the bioretention system for sustainable storm water management in urban areas. Materials & Geoenvironment, **63** (4), 227, **2016**.
18. ALMASI A., DARGAHI A., AHAGH M.M.H., JANJANI H., MOHAMMADI M., TABANDEH L. Efficiency of a constructed wetland in controlling organic pollutants, nitrogen, and heavy metals from sewage. Journal of chemical and pharmaceutical sciences, **9** (4), 2924, **2016**.
19. SHARAFI K., PIRSAHEB M., KHOSRAVI T., DARGAHI A., MORADI M., SAVADPOUR M.T. Fluctuation of organic substances, solids, protozoan cysts, and parasite egg at different units of a wastewater integrated stabilization pond (full scale treatment plant): a case study, Iran. Desalination and Water Treatment, **57** (11), 4913, **2016**.
20. MANGANGKA I.R., AN L., EGODAWATTA P., GOONETILLEKE A. Performance characterisation of a stormwater treatment bioretention basin. Journal of Environmental Management, **150** (1), 173, **2015**.
21. TAKAIJUDIN H., GHANI A.A., ZAKARIA N.A. Challenges and developments of bioretention facilities in treating urban stormwater runoff: A review. Pollution Research, **2** (4), 489, **2016**.
22. TAN Z.L., DONG Y., ARCHITECTURE S.O. Review of foreign research on pollutant bioretention technology in rain garden. Journal of Green Science and Technology, **20**, 98, **2016**.
23. MACEDO M., LAGO C., MENDIONDO E.M. Stormwater volume reduction and water quality improvement by bioretention potentials and challenges for water security in a subtropical catchment. Archives of Pharmacal Research, **647**, 923, **2019**.
24. CHOWDHURY R., KSIKSI T., MOHAMED M.M.A., ABAYA J. Performance of vegetative bioretention system

for greywater reuse in the arid climates. 8th International Conference on Environmental Science and Technology, Houston, United States of America, **2016**.
25. MINISTRY OF HOUSING AND URBAN-RURAL CONSTRUCTION OF THE PEOPLE'S REPUBLIC OF CHINA. Technical guideline for sponge city construction:construction of rainwater system with low impact development (Trial). Beijing: Ministry of Housing and Construction Rural Development, **2014** [In Chinese].
26. SUN Y.W., WEI X.M., POMEROY C.A. Global analysis of sensitivity of bioretention cell design elements to hydrologic performance. Water Science and Engineering, **4** (3), 246, **2011**.
27. YIN R.X., MENG Y.Y., ZHANG S.H., CHEN J.G. Study on runoff of bioretention by model simulation. Journal of China Hydrology, **35** (2), 28, **2015**.
28. YU G., CHOI J., HONG J., MOON S. Development and evaluation of bioretention treating stormwater runoff from a parking lot. Journal of Wetlands Research, **17** (3), 221, **2015**.
29. DAVIS A.P. Field performance of bioretention: hydrology impacts. Journal of Hydrologic Engineering, **13** (2), 90, **2008**.
30. PAN G.Y., XIA J., ZHANG X., WANG H.P., LIU E.M. Research on simulation test of hydrological effect of bioretention units. Water Resources and power, **30** (5), 13, **2012**.
31. DEBUSK K.M., HUNT W.F., LINE D.E. Bioretention outflow: does it mimic nonurban watershed shallow interflow? Journal of Hydrologic Engineering, **16** (3), 274, **2010**.
32. GULBAZ S., KAZEZYILMAZ-ALHAN C.M. Experimental investigation on hydrologic performance of LID with rainfall-watershed-bioretention system. Journal of Hydrologic Engineering, **22** (1), D4016003, **2016**.
33. GAO J.P., PAN J.K., XIE Y.C. Effects of bioretention structural layer parameters on detention and retention for road runoff. Advances in Water Science, **28** (5), 702, **2017** [In Chinese].
34. LI H., SHARKEY L.J., HUNT W.F., DAVIS A.P. Mitigation of impervious surface hydrology using bioretention in north Carolina and Maryland. Journal of Hydrologic Engineering, **14** (4), 407, **2009**.
35. LI M.H., SUNG C.Y., KIM M.H. CHU K.H. Performance of bioretention system in treating urban highway runoff: a comparison study of designs with and without an internal water storage layer. Landscape Architecture, **1**, 140, **2012** [In Chinese].
36. BROWN R.A., HUNT W.F. Hydrologic impact of an internal water storage (IWS) layer on bioretention performance. 2010 Pittsburgh, Pennsylvania, June 20 - June 23, **2010**.
37. DAVOODI R., ALMASI A., AHAGH M.M.H., DARGAHI A., KARAMI A. A mathematical model for organic matter removal in constructed wetlands case study: wastewater treatment plant of Qasr-E Shirin, Iran. International Journal of Pharmacy & Technology, **8** (2), 13155, **2016**.
38. BOANCA P.L., DUMITRAS A., LUCA L., BORS-OPRISA S. Analysing bioretention hydraulics and runoff retention through numerical modelling using RECARGA: a case study in a Romanian urban area. Polish Journal of Environmental Studies, **27** (5), 1965, **2018**.
39. MENG Y.Y., WANG H.X., Chen J.G., ZHANG S.H. Modelling hydrology of a single bioretention system with HYDRUS-1D. The Scientific World Journal, 10.1155/2014/521047, **2014**.
40. LI Z.Y., LAM K.M. Statistical evaluation of bioretention system for hydrologic performance. Water Science & Technology, **71** (11), 1742, **2015**.
41. CHEN T., LI Y., CAO K.L. Application of SUSTAIN to evaluate runoff control effect of LID practices in a residential area. China Water and Wastewater, **32** (9), 144, **2016** [In Chinese].
42. ZHANG W., SUN C., QIU Q. Characterizing of a capillary barrier evapotranspirative cover under high precipitation conditions. Environmental Earth Sciences, **75** (6), 513, **2016**.
43. GAO J.P., PAN J.K, HU N. XIE C.C. Hydrologic performance of bioretention in an expressway service area. Water Science and Technology A Journal of the International Association on Water Pollution Research, **77** (7), 1829, **2018**.
44. BOANCĂ P., DUMITRAS A., LUCA L., BORS-OPRISA S., LACZI E. Analysing bioretention hydraulics and runoff retention through numerical modelling using RECARGA: a case study in a Romanian urban area. Polish Journal of Environmental Studies, **27** (5), 1965, **2018**.
45. LINE D.E., HUNT W.F. Performance of a bioretention area and a level spreader-grass filter strip at two highway sites in North Carolina. Journal of Irrigation and Drainage Engineering, **135** (2), 217, **2009**.
46. GENUCHTEN M.T.V. A closed-form equation for predicting the hydraulic conductivity of unsaturated Soils. Soil Science Society of America Journal, **44** (5), 892, **1980**.
47. LI Y., BUCHBERGER S.G., SANSALONE J.J. Variably saturated flow in storm-water partial exfiltration trench. Journal of Environmental Engineering, **125** (6), 556, **1999**.